Journal of Ovonic Research Vol. 21, No. 5, September - October 2025, p. 667 - 673

Impact of thickness on structural and optical properties of Mno:Cuo nanostructure thin films

L. F. Hassan, F. G. Hammoodi *, M. H. Al-Timimi
Department of Physics, College of Science, University of Diyala, Iraq

Thin films of manganese oxide and copper oxide were deposited on glass substrates (2.5x2.5)cm² using chemical spray pyrolysis at 400°C. Film thicknesses varied from 150 to 550 nm with a constant 0.1 mol concentration. XRD analysis demonstrated polycrystalline films with a monoclinic structure. XRD intensity increased with thickness, and peaks shifted slightly to higher angles. FE-SEM images of the thinnest and thickest films indicate quasi-spherical nanostructures. EDX confirmed the presence of all expected elements. Optical characterization using UV-visible spectroscopy identify a decrease in transmittance and band gap with increasing thickness. Conversely, reflectance, refractive index, extinction coefficient, and real and imaginary dielectric constants increased with thickness.

(Received August 17, 2025; Accepted October 28, 2025)

Keywords: Mno:Cuo, Thin films, Optical properties, XRD

1. Introduction

The development of oxide materials plays a vital role in both chemistry and industrial applications due to their unique properties and wide range of uses. Among these materials, manganese oxide (MnO) combined with copper oxide (CuO) has garnered significant attention for its exceptional properties and versatility in fields such as electrochemistry, electronics, and magnetic materials. The ability to synthesize these oxide materials with precise control over their structure and properties is essential for optimizing their performance in various applications [1,2].

A considerable number of studies have been conducted on the effects of thickness on the structural and optical properties of MgO-doped CO_x thin films.

MnO2 doped with different percentages of nano-carbon dioxide prepared by chemical precipitation, XRD results demonstrated an increase in crystallite size with increasing doping ratio, resulting in improved thermal stability, and Optical analysis pointed decreasing energy bandgap from 7.8 eV to 6.5 eV with increasing carbon dioxide concentration [3]. The thermal calcination method used to prepare magnesium oxide samples doped with carbon dioxide (0.5-3% wt), SEM results investigate the formation of homogeneous nanoparticles with a size of 20-50 nm and an increased specific surface area [4]. The optical and structural properties of $MgO:CO_x$ prepare via electrochemical deposition method, XRD results showed a transformation of the crystal structure from cubic to hexagonal with increasing doping, and the photocatalytic efficiency improved by 40% in the analysis of organic pollutants under visible light [5].

The increasing the thickness of the $MnO_2:CO_x$ doped layer improve the light absorption in the visible region, changes in the crystal structure were detected with increasing thickness [6]. Other study identify that increasing the thickness leads to improved photovoltaic properties due to the increased concentration of nano-CO_x and decrease in the band gap with increasing thickness from 100 nm to 300 nm [7].

The thickness effect of MnO_2-CO_x films resulted in improved optical properties such as refractive index and absorption with increasing thickness and crystal structure transform from amorphous to semi-crystalline at a thickness of 200 nm [8]. Increasing the thickness of MnO_2-CO_x from 150 nm to 400 nm. improve the optical properties due to increased light scattering and the band gap decreased from 3.2 eV to 2.7 eV [9].

The structural properties enhanced due to improved nano-CO_x distribution, the absorption increase in the UV region with increasing thickness [10]. Improved structural and optical properties

* Corresponding author: faissal_hammody@uodiyala.edu.iq
https://doi.org/10.15251/JOR.2025.215.667

and increased light absorption in the visible region with increased thickness of CO_x doped on MgO_2 [11].

In this study, the MnO:CuO prepared via the chemical spray pyrolysis technique and the effect of different film thicknesses (150, 250, 350, 450, 550 nm) were investigated to obtain new improved structural and optical properties that can be used in various applications.

2. Experimental part

The chemical spray pyrolysis method used to prepare the samples due to its availability and the high acceptability of producing uniform films [12]. The structural, morphological and optical properties are investigated through XRD, FESEM, EDS and UV-visible) techniques [13,14].

The films were prepared using standard glass substrates with a thickness of (0.1 cm) and an area of (2.5×2.5) cm^2. The film's weight of MnO and CO are (1.979 g, 1.82 g) respectively. They are mixed with molarity (0.1 mol) using a magnetic stirrer at a temperature of 400°C. The prepared films thickness varies with values (150, 250, 350, 450, 550) nm.

3. Results and discussion

3.1 X-ray diffraction structure results

The structural properties for the prepared MnO:CuO films on glass substrates studied via XRD methods indicate that they are polycrystalline and monoclinic in structure (Fig. 1). The patterns of XRD pointed to the appearance of three peaks, which are (110), (002), and (-202), at the angles of 32.52°, 35.59°, and 48.74°, respectively. The dominant orientation for all the samples is (002) at an angle of 35.59° which stratify to the standard card (96-900-6674). The peaks shifted towards the right with an increase in thickness, leading to a decrease in the interplanar distance, which in turn to crystallite size decreasing (Fig1) [15]. However, the intensity increasing indicates an increasing in the degree of crystallinity that confirm with finding of [10,11].

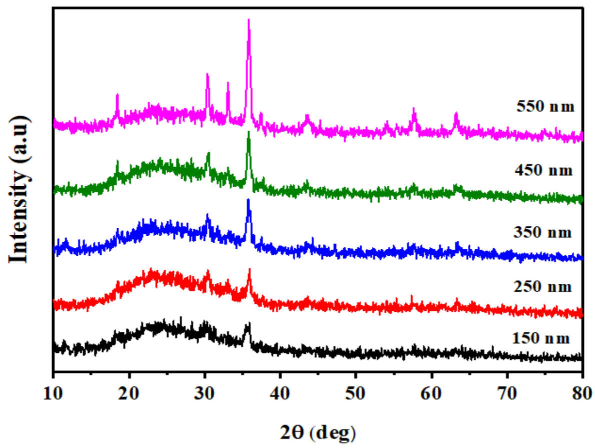

Fig. 1. XRD of MnO:CuO films at different thicknesses.

3.2. FE-SEM technique results

The morphology of the deposited materials for the prepared films using the FE-SEM was demonstrated, which has the ability to image surfaces with high resolution. The images in Figure.2 show the shapes and average sizes of the nanoparticles, which were identified through the software (Image J). In this study, two samples with the lowest and highest thicknesses were chosen for comparison. The images reveal that the films are composed of quasi-spherical nanostructured particles. Additionally, we observe that the average diameter increased with the increase in film thickness that confirm with the results of [16,17].

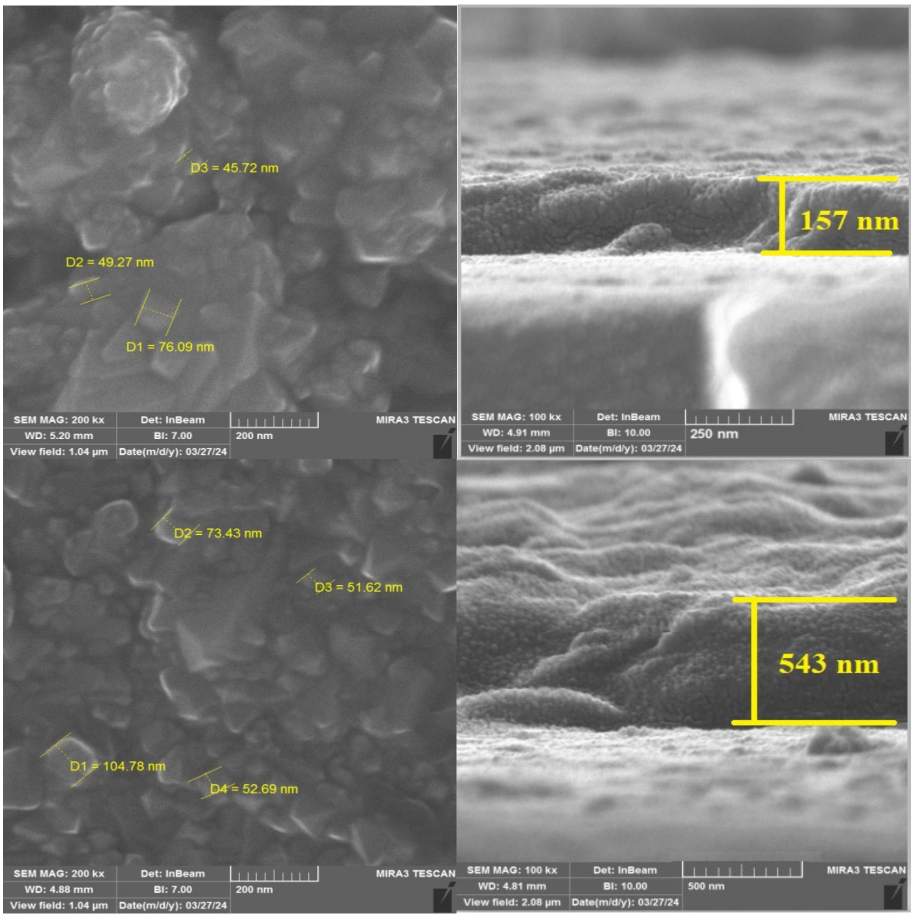

Fig. 2. FE-SEM of MnO:CuO at thickness 150 and 550 nm.

Figure 3 illustrates the Energy Dispersive Spectroscopy (EDS) spectrum and atomic structure of MnO:CuO thin films prepared at the minimum and maximum thicknesses. The results present the elemental composition of the samples, expressed as percentages. Manganese and copper are distinctly observed with four energy levels (Kα, Lα), while oxygen exhibits the Kα energy line, confirming the presence of the MnO:CuO compound. Additionally, calcium and silicon are detected at the Kα energy lines, likely originating from the glass substrate as in the finding [18].

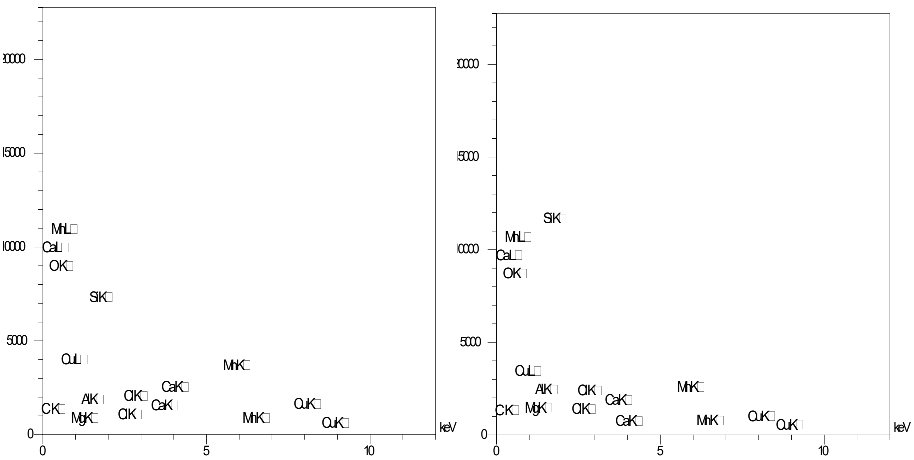

Fig. 3. EDS of MnO:CuO at thickness 150 and 550 nm

3.3. Optical properties

The transmittance spectrum of the prepared films with different thicknesses was measured as shown in (Fig.4). It is evident that the films exhibit high transmittance in the wavelength range of (300-1000) nm, where an increase in wavelength is observed in all the samples. As the thickness increases, the transmittance decreases.

We can distinguish between two regions. The first region at a thickness of 150 has an average transmittance greater than 50%, and the maximum transmittance is around 65% in the 500 nm wavelength region, as the energy of the incident photons is close to the corresponding absorption edge, which is also the fundamental absorption (500<5). The transmittance is suppressed for wavelengths less than 400 nm. This transitional wavelength range corresponds to the study of the photon energy of the formed film layers [19].

All high-energy photons are absorbed, and therefore, all photons with a wavelength less than 500 nm are transmitted. The decrease in transmittance with increasing thickness is largely dependent on the thickness, as the larger thickness leads to the phenomenon of optical absorption, and thus, a significant portion of the radiation incident on the film is attenuated [20].

Regarding reflectance, it is calculated from absorption and transmission spectra according to the law of energy conservation as expressed in equation (1). As illustrated in (Fig4), reflectance increases with increasing thickness due to the inverse relationship between reflectance and transmittance. In simpler terms, as thickness increases, reflectance increases, and vice versa that confirm with the study of [7]. The reflectance was calculated using the law of conservation of energy [21]:

$$A + T + R = 1 \quad (1)$$

where:

A: Absorptance **T:** Transmittance **R:** Reflectance

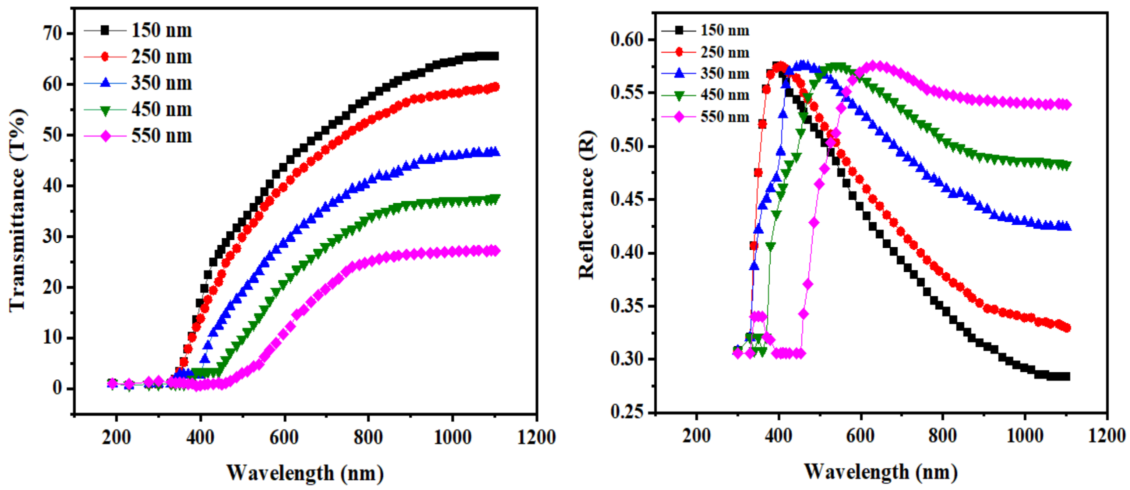

Fig. 4. Transmittance and Reflectance of MnO:CuO films.

The direct allowed energy gap of the prepared films was calculated using the following equation (2) [22,23]:

$$\alpha hv = P(hv - E_g)^r \quad (2)$$

where: **α:** Absorption coefficient, **hv:** Energy of the incident photon **P:** A constant that depends on the nature of the material, **Eg:** Optical energy gap in eV , **r:** An exponential factor that determines the nature of the electronic transition

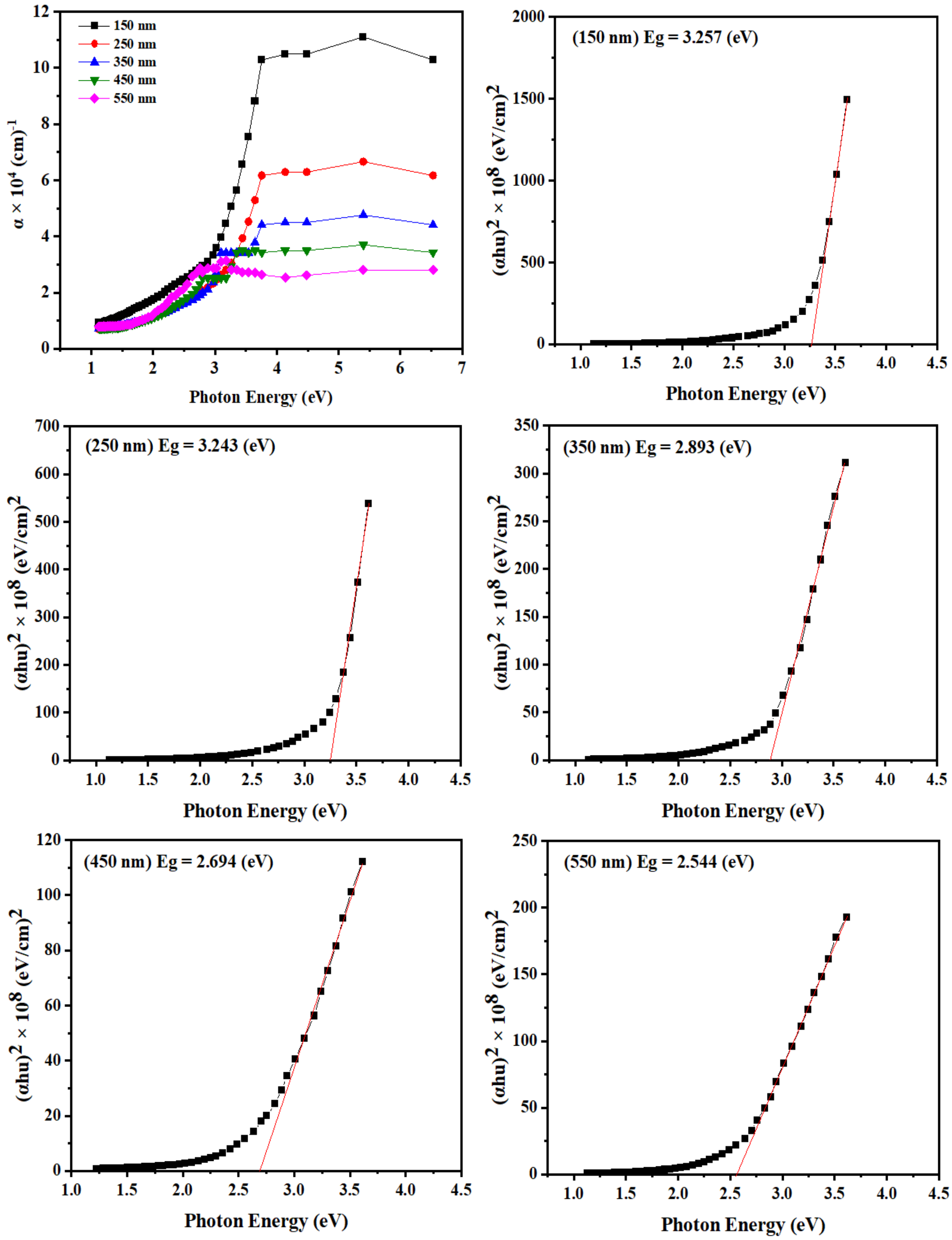

Fig. 5. The absorption coefficient and Energy gap of MnO:CuO films.

With the value of (r=1/2), it can be observed from (Fig.5) that the energy gap value decreases as the film thickness increases in the samples, because of several factors that affect the energy values, such as the deposition time and the number of the spray times, these results are aree with the finding of [3,7]. This can be attributed to the good crystallinity of our material, which imparts a large volume of the crystallites.

The refractive index is a function of the photon energy in all the prepared films with different thicknesses. It increases with increasing thickness, as the refractive index curves depend on the reflectance curves Fig. (6). the increase in the refractive index is also associated with the increase in the film density due to the improved crystalline structure of the prepared films. The extinction coefficient was calculated using the following equation (3) [24]:

$$K_o = \frac{\alpha\lambda}{4\pi} \quad (3)$$

where:

λ:Wavelength of the incident radiation in cm

The extinction coefficient is a function of the photon energy Fig. (6). It increases at low photon energies and fast increasing with high photon energies due to the absorption coefficient increasing at these energies, which indicates the occurrence of electronic transitions that agree with study of [8,9], the extinction absorption coefficients are related together that agrees with study of [25]

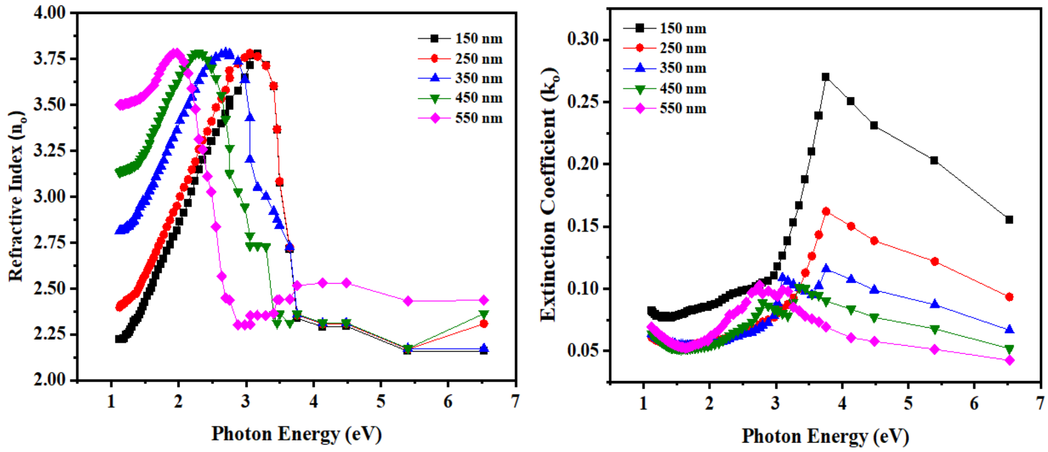

Fig. 6. Refractive index and extinction coefficient of MnO:CuO films.

4. Conclusions

This study contributes to the development of novel nanomaterials with enhanced optical properties, expanding their applications in optical and electronic devices. It also provides a basis for further research on the effects of other nano-additives on metal oxides.

The results of X-ray diffraction measurement demonstrated that the thin manganese oxide films doped with copper oxide and prepared by chemical spray pyrolysis method have a tetragonal and polycrystalline structure and the dominant trend is (101). The optical measurements identify the absorbance is within the visible spectrum, that indicates the possibility of fabrication solar cells from these films.

The results of the FESEM measurement show that the prepared films are quasi-spherical nanostructured particles. Additionally, we observe that the average diameter increased with the increase in films thickness. The optical examinations that the transmittance of the films will rise in tandem with rising doping levels, while the absorbance decreases, and the optical energy gap, absorption coefficient, and refractive index increase with increasing photon energy.

The findings from this research are contribute to understanding of the influence of thickness on the physical properties of MnO thin films, offering guidance for their application in various technological domains. Furthermore, this study will provide a foundation for future research on optimizing the nanostructured oxide materials application, ultimately enhancing their utility in scientific and industrial fields.

References

[1] R. S. Abdul-Sattar, R. S. Mohammed, L. F. Hassan, M. H. Al-Timimi, Journal of Ovonic Research **21**, 3 (2025).
[2] A. S. Zoolfakar, R. A. Rani, A. J. Morfa, A. P. O'Mullane, K. Kalantar-Zadeh, Journal of Materials Chemistry C **2**, 5247 (2014); https://doi.org/10.1039/C4TC00327D.
[3] A. M. Ali, S. H. Abdullah, Journal of Materials Science **55**, 4567 (2020); https://doi.org/10.1007/s10853-020-04476-y.
[4] A. J. Mawat, M. H. Al-Timimi, W. H. Albanda, AIP Conference Proceedings **2475**, 1 (2023),https://doi.org/10.1063/5.0103456.
[5] M. Z. Abdullah, H. M. Hasan, M. H. Al-Timimi, W. H. Albanda, M. K. Alhussainy, M. Dumitru, Journal of Ovonic Research. **15**, 199 (2019).
[6] Y. Zhang, H. Li, X. Wang, L. Chen, Journal of Materials Science **53**, 8765 (2018); https://doi.org/10.1007/s10853-018-2125-7.
[7] R. Kumar, S. Sharma, Applied Surface Science **412**, 45 (2017); https://doi.org/10.1016/j.apsusc.2017.03.210.
[8] M. H. Al-Timimi, W. H. Albanda, M. Z. Abdullah, East European Journal of Physics **2**, 173 (2023); https://doi.org/10.26565/2312-4334-2023-2-17
[9] W. H. Albandaa, M. H. Saeeda, M. Z. Abdullahb, M. H. Al-Timimic, Chalcogenide Letters **21**, 439 (2024).
[10] W. A. Aelawi, S. Alptekin, M. H. Al-Timimi, Indian Journal of Physics **97**, 3949 (2023); https://doi.org/10.1007/s12648-023-02736-6
[11] S. Patil, R. Joshi, S. Jadhav, Materials Research Bulletin **119**, 110 (2019).
[12] I. Bretos, R. Jiménez, J. Ricote, M. L. Calzada, Chemical Society Reviews **47**, 291 (2018); https://doi.org/10.1039/C6CS00917D
[13] J. D. Smith, M. L. Jones, R. E. Davis, Journal of Materials Science **50**, 1234 (2020);
[14] H. S. Al-Rikabi, M. H. Al-Timimi, I. K. Abd, AIP Conference Proceedings **2834**, 090007; (2023); https://doi.org/10.1063/5.0176417
[15] M. H. Saeed, M. H. Al-Timimi, O. Hussein, Digest Journal of Nanomaterials and Biostructures **16**, 563 (2021); https://doi.org/10.15251/DJNB.2021.162.563
[16] A. Kumar, M. Bhasin, M. Chitkara, Journal of Microscopy **292**, 123 (2023); https://doi.org/10.1111/jmi.13241
[17] A. V. Selestin, A. Karuppiah, V. G. Thanapalan, I. F. F. Christopher, Trends in Sciences **19**, 4430 (2022); https://doi.org/10.48048/tis.2022.4430.
[18] R. H. Ayoub, M. H. Al-Timimi, M. Z. Abdullah, East European Journal of Physics**3**, 546 (2023); https://doi.org/10.26565/2312-4334-2023-3-64
[19] H. Cheng, L. Chen, D. J. McClements, T. Yang, Z. Zhang, F. Ren, Z. Jin, Trends in Food Science & Technology **114**, 70 (2021); https://doi.org/10.1016/j.tifs.2021.05.017
[20] D. R. Rosseinsky, H. Lim, H. Jiang, J. W. Chai, Inorganic Chemistry **42**, 6015 (2003); https://doi.org/10.1021/ic020575s
[21] A. Y. Ibrahim, F. G. Hammoodi, Journal of Nanostructures **15**, 229 (2025).
[22] N. A. Hassan, W. H. Albanda, M. H. Al-Timimi, East European Journal of Physics **3**, 296 (2023); https://doi.org/10.26565/2312-4334-2023-3-28
[23] F. G. Hammoodi, A. A. Shuihab, S. A. Ebrahiem, AIP Conference Proceedings **2394**, 1 (2022); https://doi.org/10.1063/5.0098765.
[24] R. H. Ayoub, M. H. Al-Timimi, E. J. Lavasani, Academy of Sciences Journal **2**, 307 (2024); https://doi.org/10.24237/ASJ.02.04.791C
[25] K. T. Jadaan, F. G. Hammoodi, M. H. Al-Timimi, Nanotechnology Perceptions **20**, S3, 68 (2024).